Nature of states in a random-dimer model: Bandwidth-scaling analysis

P. K. Datta,* D. Giri,† and K. Kundu‡
Institute of Physics, Bhubaneswar 751005, India
(Received 17 February 1993)

The scaling properties of the energy spectra of a random-dimer system are studied to discern the nature of the states at and around the dimer energy (ϵ_0). The system is described by a tight-binding Hamiltonian. The scaling behavior of bandwidths for $|\ \epsilon_0\ | < 2$ shows that the system contains extended states in the neighborhood of ϵ_0. This result is further substantiated by the scaling behavior of the total bandwidth. The number of nonscattered states is found to increase with the increase in chain length. The scaling behavior of bandwidths also shows that the width of the nonscattered states depends on the dimer energy and its concentration in the sample. These results are consistent with results obtained from the transmission coefficient analysis. When the dimer energy is at the band edge ($\epsilon_0 = \pm 2$), the bandwidth scaling analysis shows that states around ϵ_0 are algebraically localized. This result is further substantiated by the behavior of the site Green function. The significance of our results in understanding the anomalous electrical conductivity in polyaniline is discussed.

I. INTRODUCTION

One of the well known results of the one-dimensional Anderson model[1] for site diagonal disorder is the absence of diffusion of an initially localized particle. This is true irrespective of the strength of the disorder.[2] The same result is equally applicable to a binary distribution even if the probability of any component is negligibly small. This result stems from the exponential localization of eigenstates in such systems. The random-dimer model[3,4] (RDM) at first sight will appear to be another example in this category. The mean square displacement of an initially localized particle in the RDM, however, grows superdiffusively in general for a significant length of time without showing any sign of saturation. This result alone makes this model an interesting subject of study. Furthermore, polymers such as polyaniline can be mapped into a RDM of its general kind.[5,6] Given the current interest in understanding the anomalous electronic transport in polymers of the kind of polyaniline,[7,8] the work of Wu and Phillips[5,6] indeed adds a new dimension to the RDM and its possible generalizations. It is, therefore, worthwhile to study this model by various techniques developed to understand the localization of eigenstates in one-dimensional systems. Our plan in the present work is to employ a technique, called bandwidth scaling,[9–15] to discern the nature of states in the RDM in the vicinity of the dimer energy. This method has already been used successfully to probe the characteristics of eigenstates in the one-dimensional Harper model[11,13] and Fibonacci crystals.[13] To our knowledge this work is the first attempt to employ the above technique in random systems such as the one under study. A brief discussion on the RDM is presented below to help the readers understand the applicability of this technique in this case.

In the context of Anderson's tight-binding Hamiltonian (TBH),[1] the RDM is described as a one-dimensional correlated random binary alloy with site energies ϵ_a and ϵ_b. The energy ϵ_a is assigned in a pair, called a dimer. It is distributed randomly in the system with probability q. All nearest neighbor hopping matrix elements are assumed to be the same in the present model. Without any loss of generality we can assign the value unity to this element. Insofar as the physically relevant parameter is the difference in site energies, we set $\epsilon_0 = \epsilon_a - \epsilon_b$ to the dimer site energies. Of course, the other site energy then has to assume the value zero. For a system containing just one dimer Dunlap, Wu, and Phillips[3] (DWP) showed that the reflection coefficient $[|\ r(E)\ |^2]$ vanishes if $E = \epsilon_0$ with $|\ \epsilon_0\ | \leq 2$. Of course, E is the incident particle energy. Further analysis,[16] albeit approximate, of the transmission coefficient $[|\ T(E)\ |^2]$ for a segment containing many dimers randomly revealed that the system contains $\sqrt{N}$ states having a localization length superior to the sample size. Here N is the number of sites in the chain under study. This analysis was further substantiated by the calculation of the Lyapunov exponent[17,18] and the density of states in the vicinity of the dimer energy. The invariant measure technique was employed to obtain the results.

The complex nature of the problem makes any rigorous analytical calculation extremely prohibitory. This, therefore, necessitates a thorough investigation of the model by numerical techniques. Sen and Gangopadhyay[19,20] along with us[21] calculated numerically the transmission coefficient of chains containing randomly placed dimers. The basic difference in these two calculations is that we implemented the basic idea of DWP from the beginning in our method. According to the first set of authors, the number of resonance states in the system goes as $N^{\frac{1}{3}}$ (Refs. 19 and 20) instead of $N^{\frac{1}{2}}$.[3–6,16] Furthermore, they claim that the superdiffusive behavior of the mean square displacement is a short time phenomenon.[20] On the other hand we obtained the following results.[21]

(i) There is a weakly configuration dependent energy width (ΔE) where $|\,T(E)\,|^2 \sim 1$. This width is found to be asymmetric around the dimer energy.

(ii) The averaged transmission coefficient yields approximately a Lorentzian curve. The half width, however, depends on the concentration (ρ) and the energy of the dimer (ϵ_0). This half width seems to scale as $N^{-\lambda}$ where λ is a function of these parameters. $\lambda \sim \frac{1}{2}$, if the concentration is large or ϵ_0 is close to one of the band edges of the host system.

(iii) Whenever $|\,\epsilon_0\,| = 2$ or infinitesimally close to this value, it appears that the states at and around the dimer energy are no longer extended. The exact nature of the states, however, cannot be discerned from the analysis of the transmission coefficient.

The analysis of the transmission coefficient, albeit necessary, is not, however, adequate to probe the nature of the states in the RDM. Note that the RDM has an energy width with the properties that (i) the states inside this width appear to be extended, and (ii) it decays with the chain length. We call this width for convenience the special spectral zone (SSZ) of the RDM. Our job is to find the number and the nature of the states in the SSZ. The number of states can be obtained from the analysis of the transmission coefficient. In principle, we can also probe the nature of the states by investigating the behavior of this quantity as a function of the chain length. If a state at a particular energy E is extended, $|\,T_N(E)\,|^2$ will be an oscillatory function of the chain length N.[22] We indeed observe such an oscillatory behavior in $|\,T_N(E)\,|^2$ in the RDM.[21] The amplitude of the oscillation, however, decays with the chain length. If the length beyond which the decay will be dominant is N_c, this quantity is found to depend on the energy probed, the energy of the dimer, and the dimer concentration in the sample. These are observed by numerical calculations. Inasmuch as the width of the SSZ in the RDM decreases with the system size, this kind of observation is expected. From this analysis one may be tempted to conclude that all states, except the one at the dimer energy, in the RDM are exponentially localized. However, it should be borne in mind that any numerical calculation has the disadvantage that one cannot probe arbitrarily close to the dimer energy. Hence, any such conclusion regarding the nature of states in the vicinity of ϵ_0 from the studies of the transmission coefficient may not be appropriate at all. One, therefore, needs a technique which will complement the transmission coefficient analysis by probing the nature of states inside the SSZ. The method of bandwidth scaling[9–15] happens to be suitable for this purpose. Since the RDM always maintains an extended state at the dimer energy,[3,4] this advantage can be exploited to employ this technique in this model. It should be apparent from this discussion that if this method is wisely blended with the analysis of $|\,T(E)\,|^2$, one can obtain a great deal of information regarding the nature of the states in the SSZ.

The organization of this article is as follows. We discuss the method empolyed here in the next section. In Sec. III we study the influence of concentration and energy of dimers on the nature of the states inside the SSZ. The nature of the states for $|\,\epsilon_0\,| = 2$ is also discussed. Section IV deals with the analysis of the site Green function. This is done to substantiate the results obtained for $|\,\epsilon_0\,| = 2$. We end the article by discussing the significance of our results in understanding the anomalous electronic transport in nonconducting polymers.[7,8]

II. FORMALISM

The RDM, mentioned earlier, is described by the well known TBH with nearest neighbor hopping only. All nearest neighbor hopping elements in this model are assumed to be unity:

$$H = \sum_l \epsilon_l\, a_l^\dagger\, a_l \;+\; \sum_l \left[a_{l+1}^\dagger\, a_l + a_{l-1}^\dagger a_l\right], \qquad (1)$$

where $a_l^\dagger$ (a_l), as usual, is the operator which creates (destroys) a particle at the lth site. The Fourier transform of the site amplitude $C_n(E)$ at any arbitrary site n for a given initial condition can be calculated by the successive application of transfer matrices[23] (P) which for the nth site is

$$P_n \;=\; \begin{bmatrix} E \;-\; \epsilon_n & -1 \\ 1 & 0 \end{bmatrix}. \qquad (2)$$

Note that the determinant of P_n, $\mathrm{Det}(P_n) = 1$, for all n. The amplitude vector $\mathbf{X}_n$ for any site n in the transposed form ($\mathbf{X}_n^T$) is

$$\mathbf{X}_n^T = (C_n(E), C_{n-1}(E)). \qquad (3)$$

Then for the $(N+1)$th site we have

$$\begin{aligned} \mathbf{X}_{N+1} &= (P_N P_{N-1} \cdots P_1)\mathbf{X}_1 \\ &= Q_N(E)\mathbf{X}_1. \end{aligned} \qquad (4)$$

The two eigenvalues of Q_N, $\Theta_\pm(N,E)$ for any N are

$$\begin{aligned} \Theta_\pm(N,E) &= \frac{1}{2}\left[\mathrm{Tr}Q_N \pm \sqrt{(\mathrm{Tr}Q_N)^2 - 4}\right] \\ &= \exp[\pm\xi(N,E)], \end{aligned} \qquad (5)$$

with Tr designating the trace of the matrix. To obtain (5) we used

$$\mathrm{Det}(Q_N) = \Theta_+\Theta_- = 1 \;\text{ for all } N. \qquad (6)$$

Furthermore,

$$\begin{aligned} \mathrm{Tr}Q_N(E) &= \Theta_+(N,E) + \Theta_-(N,E) \\ &= 2\cosh\xi(N,E). \end{aligned} \qquad (7)$$

For the perfect system when all ϵ_n's are same, $\xi(N,E) \equiv N\Phi(E)$. If $|\,\mathrm{Tr}Q_N(E)\,| > 2$, both eigenvalues Θ_+ and Θ_- are real with Θ_+ increasing exponentially with the chain length.[23] Since no physically relevant boundary condition can be satisfied, the system cannot contain any eigenstate at those energies satisfying $|\,\mathrm{Tr}Q_N(E)\,| > 2$. Hence, there will be spectral gaps at those energies. On the other

hand if $|\ \mathrm{Tr}Q_N(E)\ | < 2$, both eigenvalues are complex with $|\ \Theta_{\pm}(N,E)\ | = 1$. The solution vector $\mathbf{X}_{N+1}$ cannot grow in this situation. It is, therefore, possible to satisfy physically acceptable boundary condition at those energies for which $|\ \mathrm{Tr}Q_N(E)\ | < 2$. Energies satisfying $|\ \mathrm{Tr}Q_N(E)\ | = 2$ separate these two regimes.

Consider a chain containing N sites. All the site energies (ϵ_n) in this chain may or may not be identical. Treating this chain as the unit cell we construct a ring comprising of M such units. The amplitude equation for the $(NM+1)$th site is

$$\begin{aligned}\mathbf{X}_{NM+1} &= [Q_N(E)]^M \mathbf{X}_1 \\ &= [U^{-1}T(M,N,E)U]\mathbf{X}_1, \end{aligned} \tag{8}$$

with

$$T(M,N,E) = \begin{bmatrix} \exp[M\xi(N,E)] & 0 \\ 0 & \exp[-M\xi(N,E)] \end{bmatrix}. \tag{9}$$

U is the matrix that diagonalizes $Q_N(E)$. To satisfy the prescribed periodic boundary condition we need

$$\begin{aligned}\mathrm{Tr}Q_N(E) &= 2\cosh\xi(N,E) = 2\cos\frac{2\pi n}{M}, \\ &\text{with } n = 0, \pm 1, \pm 2, \ldots, \pm\frac{M}{2}. \end{aligned} \tag{10}$$

Inasmuch as there are (MN) eigenstates in the present system with the property

$$\epsilon_{n\pm N} = \epsilon_n, \tag{11}$$

it must contain N bands and $(N-1)$ gaps. The bands are, of course, characterized by the energy widths satisfying $|\ \mathrm{Tr}Q_N(E)\ | \leq 2$.[9]

Since the eigenstates of this superlattice extend over the whole sample, at the unit cell level states appearing at those energies must be extended for any finite value of N.[9] Of course, they are not necessarily of the Bloch type at the unit cell level. However, in the limit $N \to \infty$, the effect of the superlattice structure on the unit cells will disappear. So the states which are extended for a given value of N may undergo localization as N increases. To understand how the extended states are changing the characteristics, it is necessary to investigate the scaling behavior of the isomorphic bands with N. It is a case of multifractal analysis and is described below. This method has one important advantage. Site amplitudes in the unit cell are allowed to develop freely in this mode of analysis. This is the appropriate boundary condition for infinite systems. Many important and interesting results can be obtained by investigating the system this way.[15]

The basic idea in the multifractal analysis is to partition a given set in a prescribed way. The next stage in the analysis is to attach a Lebesgue measure (Δ_i) and a probability measure (p_i) to each of the partitioned subsets. One can then obtain criteria for the localization of states in a given sample by examining the scaling properties of either the Lebesgue measure (Δ_i) or the probability measure (p_i). The details can be found in Ref. 13. The set in the present example is the total allowed spectral region. The band structure generates the desired partitioning. p_i here is a constant, namely, $\frac{1}{N}$. N is number of sites in the system of interest. Δ_i $(i = 1, 2, \ldots, N)$ is the width of the ith band. The nature of the states in the allowed spectral region can be obtained from the asymptotic scaling behavior of the bandwidths with chain length (N). The scaling criteria[9–15] for identifying the nature of states are presented below with examples.

(i) If $\epsilon_{n\pm N} = \epsilon_n$, we have N bands characterized by $|\ \mathrm{Tr}Q_N(E)\ | \leq 2$. We also have $(N-1)$ gaps.

(ii) If a band decays exponentially with the chain length, states in that energy width are exponentially localized.

Consider the case $\epsilon_n = \lambda\tan[2\pi(n\omega - \nu)]$ and $\omega = \frac{p}{q}$. p and q are integers. Bands in this example have widths proportional to $e^{-\gamma N}$ $(\gamma > 0)$ irrespective of the value of λ. All states in this sample are exponentially localized.[24]

(iii) If a band scales as $N^{-\alpha}$ and $\alpha = 1$, the states in the band are extended. If $\alpha > 1$, states are critical.

This behavior is beautifully exemplified by the Harper model characterized by $\epsilon_n = \lambda\cos(2\pi n\omega)$ where ω is an irrational number.[11,13] If $\lambda < 2$, each bandwidth scales as $\frac{1}{N}$ except the ones at the ultimate spectral boundaries. The width of the bands there goes as $\frac{1}{N^2}$. All states are, therefore, extended. If $\lambda = 2$, each bandwidth is proportional to $\frac{1}{N^\alpha}$, $\alpha > 1$. So states are critical. In Fibonacci crystals also one finds bandwidths scaling as $\frac{1}{N^\alpha}$, $\alpha > 1$.[13] It is well known that states are critical in Fibonacci crystals.[18]

The successful implementation of the bandwidth scaling method requires identification of isomorphic bands in the successive partitioning of the total allowed spectral region. The Harper model and Fibonacci crystals generate bands in a regular way to form Cantor set spectra.[13] So these models can be studied successfully by this method. On the other hand, in a purely random system the fragmentation of the bands does not follow any prescribed rule. Consequently, the scaling of individual bands in such a system is not possible. In this respect, the RDM is unique due to the presence of a nonscattered state at the dimer energy. So there must be an energy width for all N around the dimer energy where $|\ \mathrm{Tr}Q_N(E)\ | \leq 2$. This band can be used as a reference to number the bands in the system. For example, its nearest neighbors can be called (1′) or (1) depending on whether the band is towards the nearest band edge of the parent system or not. Similarly, we can number other bands as (2′), (2), (3′), (3), etc. We can, therefore, exploit this advantage to employ the bandwidth scaling method here to discern the nature of states.

We end this section by discussing the utility of the scaling of the total bandwidth (B_T).[9,10,14] It is well known that almost all states are exponentially localized in a totally random system. So B_T in such systems must decay exponentially with N.[10,14] On the other hand, if $B_T \propto N^{-\beta}$, $\beta > 0$, we must conclude that the system contains states which are either extended or algebraically localized. Consider now the RDM. Since it contains site diagonal disorder, one would expect that B_T in

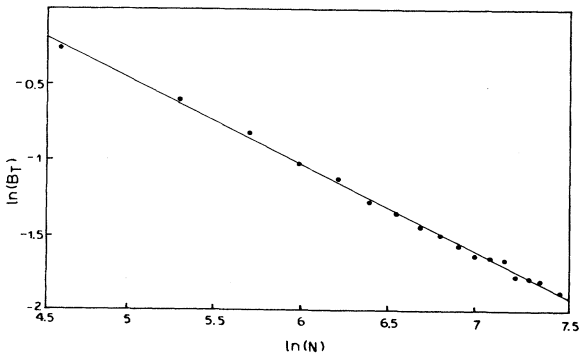

FIG. 1. The log-log plot of the total bandwidth (B_T) with N. The dimer energy $\epsilon_0 = 0.8$ and concentration $\rho = 0.33$. The solid line corresponds to the least squares fit of the data points. The fitting curve is obtained as $\ln B_T = \ln C - \beta \ln N$, where $C \sim 11.01$ and $\beta \sim 0.57$.

this model will decay exponentially with N. B_T, however, scales as $N^{-0.57}$ for $\epsilon_0 = 0.8$ and $\rho = 0.33$ (Fig. 1). Since this value of the exponent resulted from relatively small sample sizes, it is an approximate value. However, it should be noted that the obtained value is in quite good agreement with 0.5 obtained by DWP.[3] Inasmuch as the scaling result for B_T points out that all states in the RDM are not exponentially localized, we, therefore, examine next the scaling of individual bands at and around the dimer energy (ϵ_0).

III. RESULTS AND DISCUSSION

We first present the scaling behavior of the band around ϵ_0. The width of this reference band (Δ_0) is plotted against the chain length (N) in the log-log plots for various values of ϵ_0. Data points are found to obey

$$\ln \Delta_0 = \ln C_0 - \alpha_0 \ln N. \tag{12}$$

Results are presented in Figs. 2(a)–2(c). The values of α_0 and C_0 for different values of ϵ_0 are also listed in Table I. Since every investigation of the RDM suggests that

TABLE I. The value of C and bandwidth scaling index (α) of the reference band for different dimer energies (ϵ_0). Concentration of dimers $\rho = 0.33$.

Dimer energy (ϵ_0)	C_0	α_0
0.001	6.28107	0.999979
0.8	5.27411	0.991917
1.98	0.70467	0.977748

the state at ϵ_0 is extended, we should expect $\alpha_0 \to 1$ as $N \to \infty$. When ϵ_0 is well inside the parent band, the desired asymptotic value of α_0 is obtained for N not exceeding 10^5. However, for $\epsilon_0 = 1.98$ we obtain $\alpha_0 \sim 0.98$ in the investigated range of N. This value is, of course, perceptibly away from the desired asymptotic value. This can be explained by noting that $\epsilon_0 = 1.98$ is very close to one of the band edges of the host system. It is well known that states near the band edges have high propensity towards localization in the presence of disorder. Hence, to obtain the desired asymptotic value of α_0, larger values of N will be needed. This explanation is further supported by the scaling behavior of adjacent bands for $\epsilon_0 = 1.98$. We present the scaling behavior of (1) and (1′) bands in Figs. 3(a) and 3(b). Note that the band which is away from the band edge shows better scaling behavior in the investigated range of N.

Since the value of N beyond which the reference band shows the expected scaling behavior depends on ϵ_0, the width of the nonscattered states must also depend on this quantity. This dependence is beautifully exhibited in the scaling behavior of the bands around the dimer energy for $\epsilon_0 = 0.001$ and 0.8. The concentration of the dimer ($\rho = 0.33$) in the chain is same in both cases. The scaling behavior of (2), (5) and (2′), (5′) bands for these energies are shown in Figs. 4(a)–4(d) and Figs. 5(a)–5(d), respectively. The values of α_i and C_i are also given in Table II and Table III. We find that for $\epsilon_0 = 0.001$, the desired asymptotic value of α_i is obtained for relatively small values of N. Furthermore, for this value of ϵ_0, values of α and C show no dispersion in the investigated

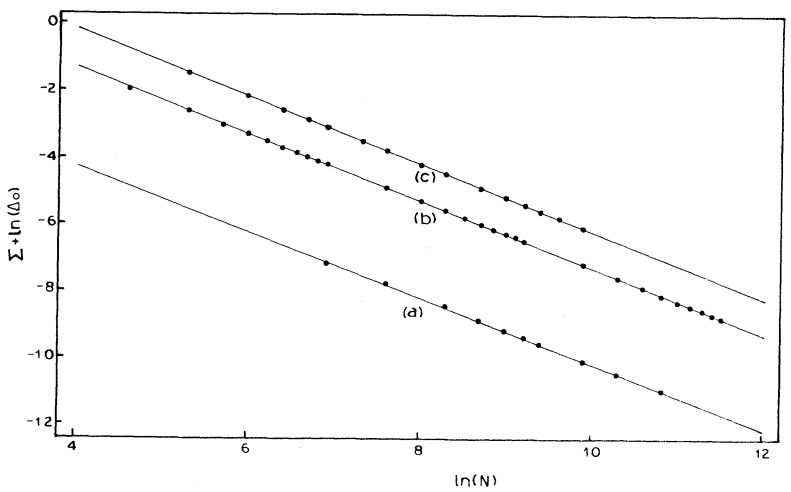

FIG. 2. The log-log plot of the width (Δ_0) of the reference bandwidth N. Note that one constant Σ is added to the ordinate for clarity. The value of Σ increases every time by one unit as we go up from the bottom figure. (a) The dimer energy $\epsilon_0 = 1.98$, concentration $\rho = 0.33$, and $\Sigma = 0$. The least squares fit (solid line) obtained as $\ln \Delta_0 = \ln C_0 - \alpha_0 \ln N$. Values of C_0 and α_0 are given in Table I. (b) Same as (a) but $\epsilon_0 = 0.8$ and $\Sigma = 1$. (c) Same as (a) but $\epsilon_0 = 0.001$ and $\Sigma = 2$.

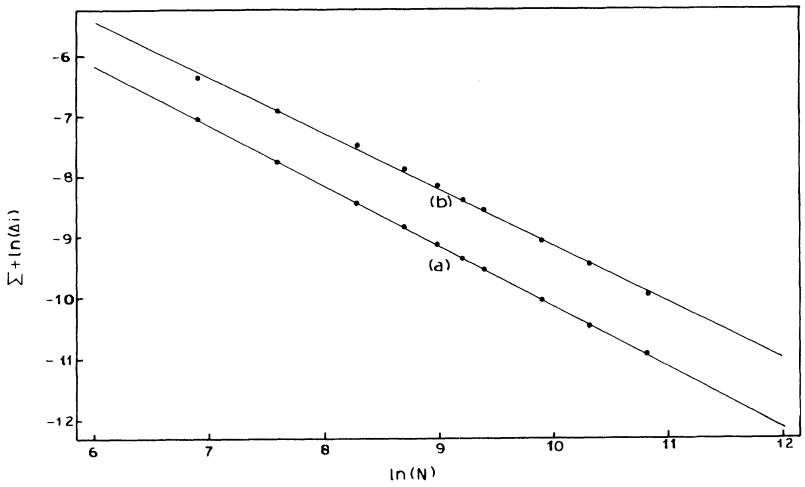

FIG. 3. (a) The log-log plot of the bandwidth (Δ_i) having index $i = 1$ with N. The dimer energy $\epsilon_0 = 1.98$, $\rho = 0.33$, and $\Sigma = 0$. The least-squares fit (solid line) of the data points yields $\ln\Delta_1 = \ln C_1 - \alpha_1 \ln N$, where $C_1 \sim 0.845$ and $\alpha_1 \sim 0.997$. (b) Same as (a) but band index $i = 1'$ and $\Sigma = 1$. Here $C_{1'} \sim 0.425$ and $\alpha_{1'} \sim 0.928$.

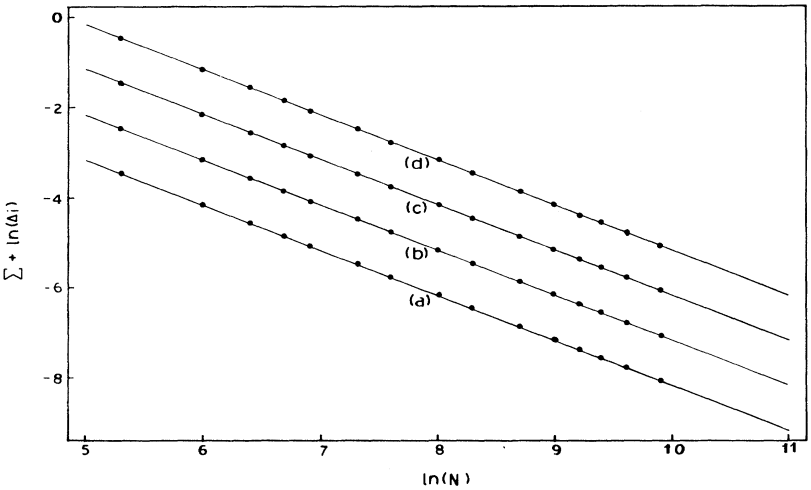

FIG. 4. The log-log plot of the bandwidth (Δ_i) with N. (a) The dimer energy $\epsilon_0 = 0.001$, $\rho = 0.33$, band index $i = 2$, and $\Sigma = 0$. (b) Same as (a) but band index $i = 5$ and $\Sigma = 1$. (c) Same as (a) but band index $i = 2'$ and $\Sigma = 2$. (d) Same as (a) but band index $i = 5'$ and $\Sigma = 3$.

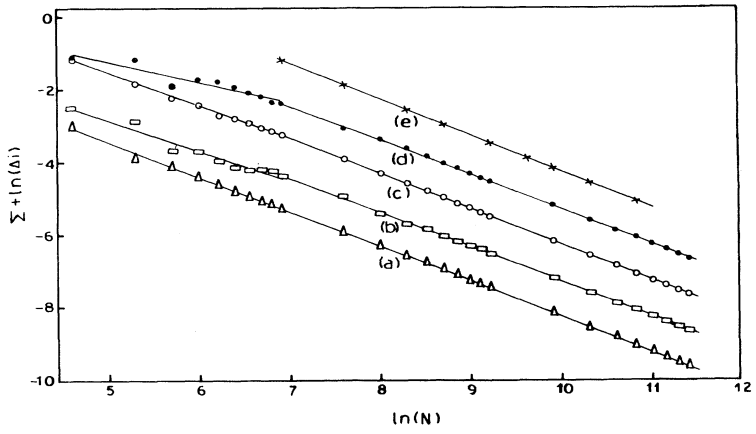

FIG. 5. The log-log plot of bandwidth (Δ_i) with N. (a) Here $i = 2$, $\epsilon_0 = 0.8$, $\rho = 0.33$, and $\Sigma = 0$. The least squares fit (solid line) is shown for three different regions of N, (i) $10^2 - 10^3$, (ii) $10^3 - 10^4$, (iii) $10^4 - 10^5$. (b) Same as (a) but band index $i = 5$ and $\Sigma = 1$. (c) Same as (a) but band index $i = 2'$ and $\Sigma = 2$. (d) Same as (a) but band index $i = 5'$ and $\Sigma = 3$. (e) Same as (b) but $\rho = 0.01$ and $\Sigma = 4$. The least squares fit (solid line) of the data points shows the behavior as $\ln\Delta_5 = \ln C_5 - \alpha_5 \ln N$, where $C_5 \sim 5.374$ and $\alpha_5 \sim 0.994$.

TABLE II. The value of C and bandwidth scaling index (α) of different bands for dimer energy $\epsilon_0 = 0.001$ and concentration $\rho = 0.33$.

Band index (i)	C	α
2	6.2562	0.999695
2′	6.2574	0.999655
5	6.2517	0.999643
5′	6.2473	0.999554

range of N. On the other hand, to obtain stable values of α and C for $\epsilon_0 = 0.8$, larger values of N are needed. This observation suggests that the width of the nonscattered states for $\epsilon_0 = 0.001$ is larger than the corresponding width for $\epsilon_0 = 0.8$. Our scaling result is also corroborated by the analysis of the transmission coefficient. The plots of the transmission zone for these two values of ϵ_0 and $N = 10^5$ are presented in Fig. 6(a) and Fig. 6(b) for comparison. This result can be explained by considering the effect of scattering on a given energy (E) state due to dimer impurities. Scattering depends on two quantities, the magnitude of ϵ_0 and its distance from ϵ_0, that is, $\mid E-\epsilon_0 \mid$. When ϵ_0 is large, scattering is also large. Similarly if $\mid E-\epsilon_0 \mid$ is large, a given band may not be in the SSZ for a certain range of N. However, if N increases, this band will eventually move into the SSZ where the scattering effect vanishes. Of course, this can only happen if the SSZ in the RDM does not decay exponentially with N. Hence, any increase in ϵ_0 will require a decrease in $\mid E-\epsilon_0 \mid$ to overcome the effect of scattering. Inasmuch as the number of bands that will enter the SSZ decreases with the increase in ϵ_0, the width of the nonscattered states in the RDM must decrease with increasing ϵ_0.

That the effect of scattering from dimer impurities on a given band depends on $\mid E-\epsilon_0 \mid$ can be observed in the scaling behavior of bands for a given ϵ_0 and concentration (ρ). Consider the scaling of bands for $\epsilon_0 = 0.8$ and $\rho = 0.33$. Our results are as follows.

(i) Bands do not exhibit any scaling behavior for small values of N.

(ii) The value of N beyond which a given band exhibits a well defined scaling behavior depends on the index of the band. This value of N increases with the index of the band.

(iii) The values of α and C depend on the range of N. Furthermore, because of randomness in the system these quantities do not obey any well defined pattern in a certain range of N. The value of N, of course, depends on the band index.

(iv) As $N \to \infty$, $\alpha \to 1$ and C attains a stable value. This is true for all bands.

(v) In a given range of N the value of the scaling amplitude (C) decreases as the distance of a band from the reference band increases.

The effect of scattering due to dimer impurities and the influence of the SSZ on a given band need to be considered to explain these results. Note that scattering will play an important role until a given band enters the SSZ. Because of this scattering, the bandwidth will not decrease systematically with N. So no well defined scaling behavior will be observed. This band will, however, enter the SSZ if N exceeds a certain value. Then the effect of scattering will reduce. Hence a well defined scaling behavior will be observed. But the value of α will not be unity in general. This band will move further inside the SSZ with further increase in N. When it moves well inside the SSZ, it is totally shielded from scattering. We then obtain $\alpha = 1$ and a stable value of C. Furthermore, the approach of α asymptotically to unity from below suggests that randomness introduces nonlinear decay in bandwidths for finite values of N. In addition, the algebraic decay of the SSZ with N has another important consequence. Any band with finite index (i) will eventually enter the SSZ. However, the value of N beyond which the band moves into the SSZ diverges with i. So the range of N in which no well defined scaling behavior is obtained also diverges. This is observed in our analysis. The critical value of i beyond which no band can effectually enter the SSZ can be estimated from the scaling of the total bandwidth. This will yield an estimation of the nonscattered states in the system for a given value of N. Furthermore, the absence of a well defined regime separating the extended states from the localized ones explains the observed decrease of C_i as band index i increases.

The effect of ρ on the width of the nonscattered states is also examined, albeit not elaborately. The result for $\rho = 0.01$ and $\epsilon_0 = 0.8$ is presented in Fig. 5(e). Inasmuch as the reduction in the concentration of the dimers will reduce the effect of scattering, any given band should exhibit $\frac{1}{N}$ behavior for relatively small values of N. This is actually observed. Compare Fig. 5(b) and Fig. 5(e).

TABLE III. The value of C and bandwidth scaling index (α) of different bands in different range of N. The dimer energy $\epsilon_0 = 0.8$ and concentration $\rho = 0.33$.

Range of N	$10^2 - 10^3$		$10^3 - 10^4$		$10^4 - 10^5$	
Band index (i)	C	α	C	α	C	α
2	4.070	0.968	3.791	0.956	5.493	0.996
2′	2.699	0.904	4.685	0.979	5.216	0.992
5	1.299	0.825	3.364	0.949	4.334	0.976
5′	0.231	0.556	2.667	0.921	4.804	0.987

We also investigated the scaling behavior of gaps. For none of the gaps did we obtain any well defined scaling behavior. However, gaps adjacent to the reference bands did not show any indication of exponential decay with N. This observation, albeit not conclusive, suggests that states around ϵ_0 are not exponentially localized.

We showed in our previous work[21] that the nature of state at ϵ_0 when $\epsilon_0 = \pm 2$ cannot be discerned by the analysis of the transmission coefficient. The method of bandwidth scaling can be applied successfully in this case. Results are presented in Figs. 7(a)–7(c). The values of α and C for various bands are shown in Table IV. The scaling results suggest that states at and around ϵ_0 for $\epsilon_0 = \pm 2$ are critical like. To substantiate this result we examine the Green function of a one-dimensional chain containing dimers randomly. Before leaving this section we emphasize that all results have been checked with more than one sample. Here we only presented the typical results. Furthermore, all quantities that are plotted are dimensionless.

IV. SITE GREEN FUNCTIONS ANALYSIS

We analyze the site Green functions for a one-dimensional chain containing dimer impurities randomly. The relevant TBH (H) for this system has already been discussed in Sec. II. The Green function in the operator form is

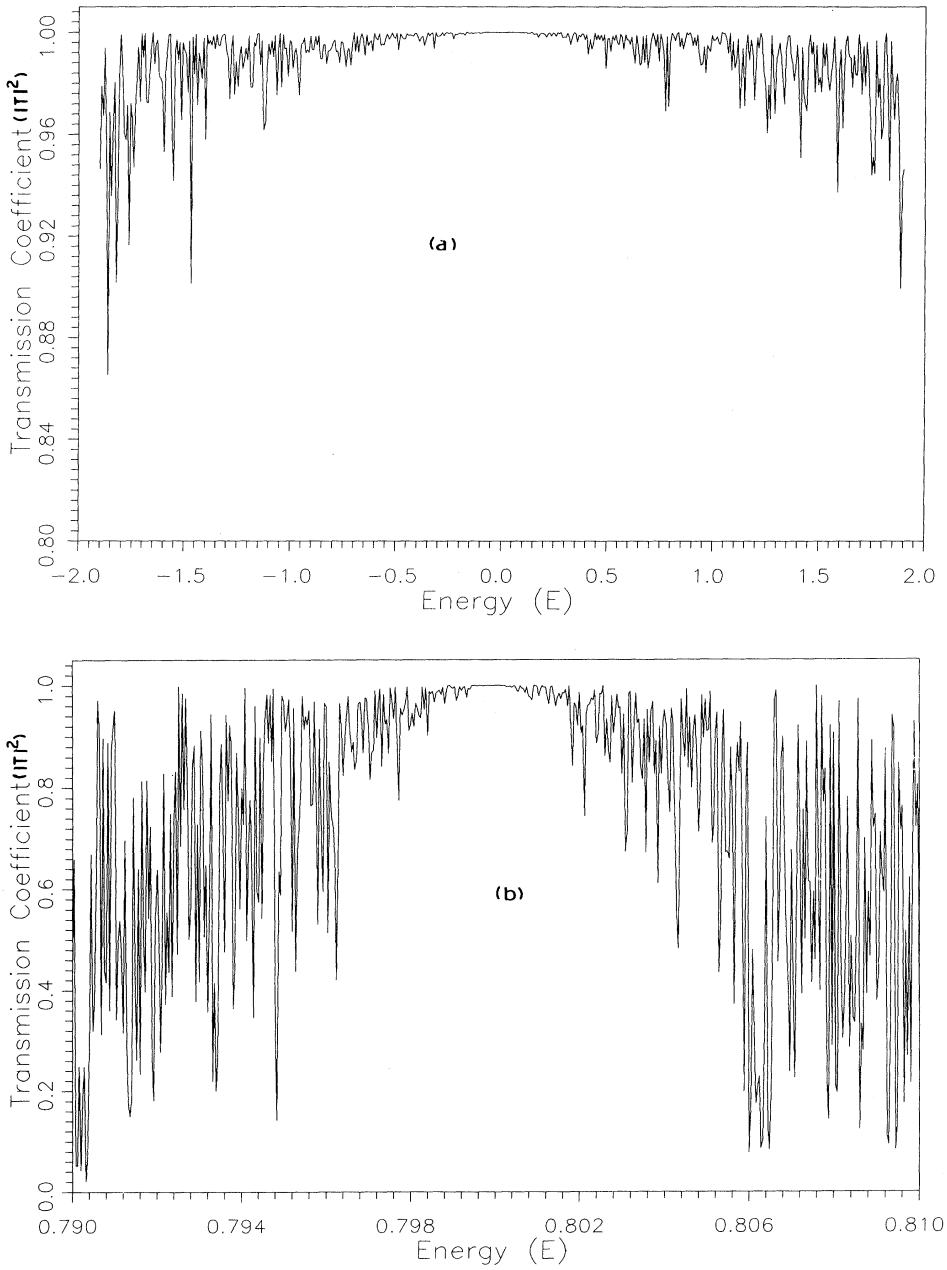

FIG. 6. Plot of transmission coefficient ($|T|^2$) as a function of the particle energy (E) for the RDM with sample length $N = 10^5$. The dimer energy $\epsilon_0 = 0.001$ and the concentration $\rho = 0.33$. (b) Same as (a) but $\epsilon_0 = 0.8$.

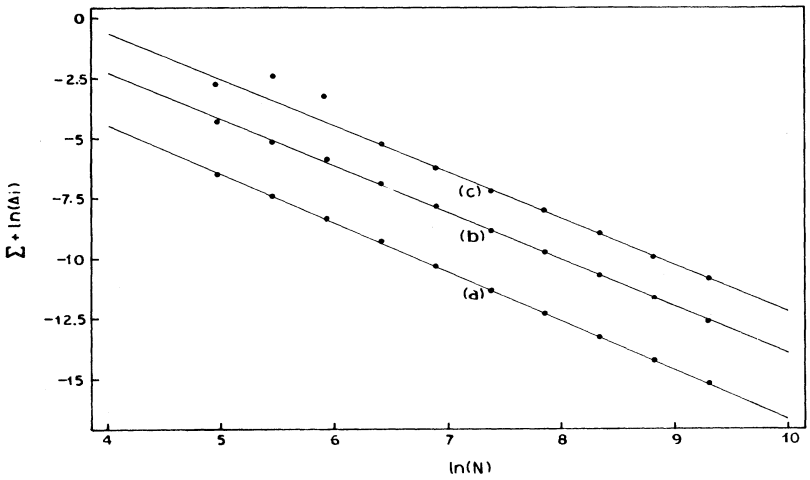

FIG. 7. The log-log plot of bandwidth (Δ_i) with N, where (a) $i = 0$, $\epsilon_0 = 2.0$, $\rho = 0.33$, and $\Sigma = 0$. (b) Same as (a) but $i = 2$ and $\Sigma = 1$. (c) Same as (a) but $i = 5$ and $\Sigma = 2$.

$$G(z) = (z - H)^{-1}, \tag{13}$$

where z is a complex parameter. The properties of the system are obtained from the analysis of $G(z)$ along the real line. The real value of z is given by E, the energy under investigation. Inasmuch as detailed analysis of the site Green function can be found in the literature,[25] we discuss in bare details the behavior of $G(z)$ for the system under consideration.

We consider first the simplest possible case. This is the case of the perfect system containing only one dimer with dimer energy ϵ_0. Since a dimer is equivalent to two substitutional impurities with equal strength occupying nearest neighbor sites, say, l and m, the Green function for this system is

$$G(z) = G_{0,l}(z,\epsilon_0) + G_{0,l}(z,\epsilon_0) \mid m\rangle \frac{\epsilon_0}{1 - \epsilon_0 G_{0,l}(m,m,z,\epsilon_0)} \langle m \mid G_{0,l}(z,\epsilon_0), \tag{14}$$

where

$$G_{0,l}(m,m,z,\epsilon_0) = \langle m \mid G_{0,l}(z,\epsilon_0) \mid m\rangle.$$

$G_{0,l}(z,\epsilon_0)$ is the single-impurity Green function for the system containing a substitutional impurity of strength ϵ_0 at the lth site. The poles of the Green function under investigation are obtained from

$$G_{0,l}(m,m,E_p,\epsilon_0) = \frac{1}{\epsilon_0}. \tag{15}$$

Since the poles of $G(z)$ correspond to discrete eigenvalues of the Hamiltonian under consideration, E_p must be real. Furthermore, if $\mid \epsilon_0 \mid < 2$, only one discrete level outside the parent band is obtained. However, for $\mid \epsilon_0 \mid = 2$, we obtain two poles. This is illustrated in Fig. 8(a) for $\epsilon_0 = 2$. If we take $\epsilon_0 = -2$, we obtain the mirror image of Fig. 8(a). Note one discrete level is always outside the band at $E_{p1} = \frac{10}{3}$. The most significant aspect, however, is the appearance of a second pole exactly at $E_{p2} = 2$.

If we take $\epsilon_0 = 2 + \delta$ and $\delta > 0$, for small values of δ, we obtain $E_{p2} \sim 2 + \delta^2$. Since E_{p2} is outside the parent band, states at that energy must be exponentially localized. This should be true even if δ is vanishingly small. On the other hand, this pole disappears if $\delta < 0$. So, for $\delta < 0$, this state becomes extended. Since a state cannot suffer such an abrupt change in nature in a small energy neighborhood, we argue that the state at E_{p2} for $\epsilon_0 = 2$ is neither extended nor localized. In other words, it must be algebraically localized. If the state at E_{p2} for $\epsilon_0 = 2$ is indeed exponentially localized, we must obtain a δ function singularity in the density of states. Instead we obtain the following results.

(a) When $\epsilon_0 = 2$, the imaginary part of $G_{0,l}(m,m,E,\epsilon_0)$ vanishes at $E = 2$ which is shown in Fig. 8(a). $G_{0,l}(m,m,E,\epsilon_0)$ is the Green function at the mth site with the impurity at the lth site.

(b) The imaginary part of the two-impurity Green function around $E = 2$ diverges as $(2 - E)^{-1/2}$ [Fig. 8(a)]. Note that the local density of states for perfect systems also exhibits the same kind of divergence at the band edges. These observations are consistent with the intermediate nature of the state at $E = 2$, when $\epsilon_0 = 2$.

We next study a system containing more than one dimer. Our procedure to calculate the relevant site Green function is as follows.

(i) We take a chain of size N. The chain contains many dimers randomly with a given concentration (ρ).

TABLE IV. The value of C and bandwidth scaling index (α) of different bands for dimer energy $\epsilon_0 = 2.0$ and $\rho = 0.33$.

Band index (i)	C	α
0	40.839	2.0367
2	99.176	1.95351
5	191.115	1.92707

(ii) We attach this chain to perfect systems of infinite length at both end points.

(iii) This chain of interest always contains a dimer at one end. We calculate the Green function for this end point. This gives us the actual site Green function.

(iv) We replace next that site of the dimer which is at the end point under consideration by a perfect site.

(v) We calculate the Green function for this altered system at the site of interest using the renormalized perturbation expansion (RPE) method.[25] We denote this Green function as $\tilde{G}$.

(vi) The actual Green function is calculated then by using the technique to calculate this function for a single impurity.

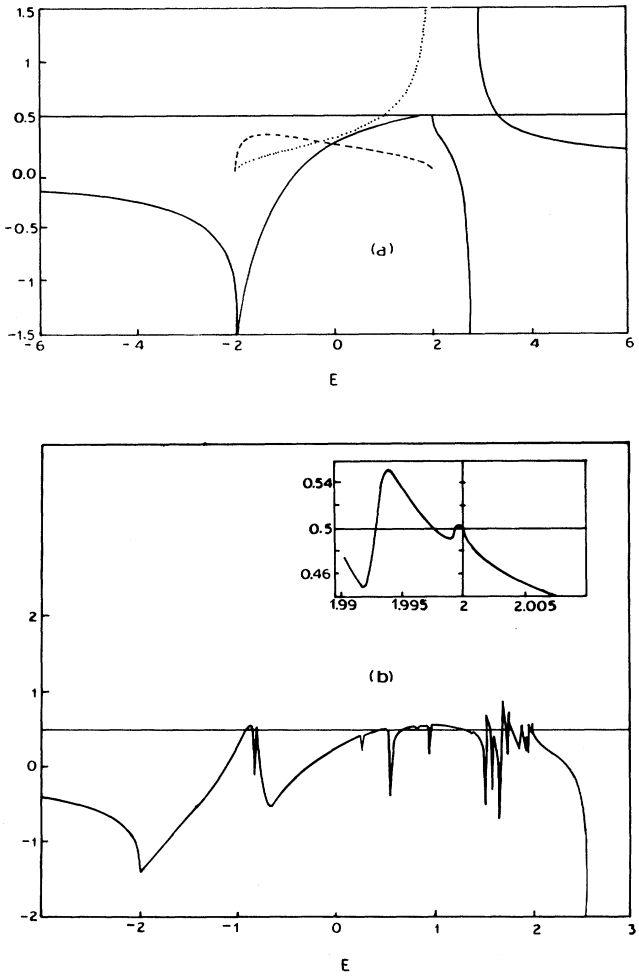

FIG. 8. (a) The solid curve corresponds to the real part of $G_{0,l}(m,m,E,\epsilon_0)$ as a function of E. The solid straight line corresponds to $G_{0,l}(m,m,E,\epsilon_0)=\frac{1}{\epsilon_0}$. The dashed curve corresponds to the imaginary part of $G_{0,l}(m,m,E,\epsilon_0)$. The dotted curve corresponds to the local density of states. All curves are drawn for $\epsilon_0=2$. (b) The real part of $\tilde{G}(m,m,\epsilon_0,E)$ as a function of E which is represented by the solid curve and the straight line corresponds to $\tilde{G}(m,m,\epsilon_0,E)=\frac{1}{\epsilon_0}$. Here $\epsilon_0=2.0$ and $\rho=0.33$. The inset shows details of the curve $\tilde{G}(m,m,\epsilon_0,E)$ with E and $\tilde{G}(m,m,\epsilon_0,E)=\frac{1}{\epsilon_0}$ around $E=\epsilon_0=2.0$.

Let m be the site of interest. If E_p is the pole of the actual Green function, it is obtained from

$$\tilde{G}(m,m,\epsilon_0,E_p)=\frac{1}{\epsilon_0}, \tag{16}$$

when

$$\tilde{G}(m,m,\epsilon_0,E)=\frac{1}{E-\Delta(m,m,\epsilon_0)}. \tag{17}$$

$\Delta(m)$ is the self-energy and is given by

$$\Delta(m)=G(m-1,m-1,[m])+G(m+1,m+1,[m]).$$

Here $G(m-1,m-1,[m])$ is the Green function at the site $(m-1)$ with the site m is excluded. The real part of the Green function $\tilde{G}(m,m,\epsilon_0,E)$ is shown in Fig. 8(b) for $\epsilon_0=2$, $\rho=0.33$, and $N=100$. Note again the Green function has a pole at $E=2$ when $\epsilon_0=2$. Also it can be shown that the local density of states diverges as $(2-E)^{-1/2}$. Hence, the nature of the state at $E=2$ for $\epsilon_0=2$ does not change by changing the number of dimers in the system. This result is also consistent with the results obtained from the scaling behavior of the bandwidths. Note that the scaling analysis yielded $\alpha\sim 2.03$ for the band at $\epsilon_0=2$. Also, the value of the scaling parameter (α) for other bands is much larger than 1. All these results together prove that the states around the dimer energy for $\epsilon_0=2$ are critical like.

V. CONCLUSION

We employed a technique, called bandwidth scaling, to discern the nature of states in the special spectral zone, present in the RDM. The observed scaling behavior of the total bandwidth (B_T) is consistent with the presence of states which are not exponentially localized. Furthermore, the bands at and around ϵ_0 for $|\epsilon_0|<2$ yield unity to a fair degree of accuracy for the scaling exponent α. Since an extended state is characterized by $\alpha=1$, we conclude that the system contains extended states in the neighborhood of ϵ_0. Furthermore, the effect of scattering on the states due to dimer impurities is also amply evident in the scaling behavior of the bands. For any given band we find that no definite scaling behavior is obtained unless the value of N exceeds a certain value. This range of N, albeit not well defined, increases with increasing the band index (i), the dimer energy (ϵ_0), and the concentration of dimers (ρ) in the sample. The dependence of this range on ϵ_0 and ρ suggests that the width of the nonscattered states in the RDM depends on these quantities. We obtained similar results previously by investigating the transmission coefficient. Since all bands show the tendency to enter the SSZ, we conclude that number of states in the SSZ increases as N increases. However, it should be borne in mind that B_T decreases algebraically with N. Hence, all bands cannot enter the SSZ. The number of nonscattered states can be estimated from the scaling behavior of B_T. This is consistent to a fair degree

with the results of DWP.

When the dimer energy is at the band edge ($\epsilon_0 = \pm 2$), the picture is quite different. States at and around ϵ_0 are no longer extended. This is clearly seen in the scaling behavior of bands in the neighborhood of ϵ_0. The observed scaling behavior suggests that states are critical. The behavior of the site Green function supports this inference.

Since Wu and Phillips showed that polymers such as polyaniline can be mapped into a random dimer problem, the dependence of the width of nonscattered states on ϵ_0 should not be belittled. This may be the key to the understanding of anomalous electrical conductivity in polymers, such as polyaniline. Polyaniline shows anomalous electrical conductivity upon oxidation and protonation. The oxidation reaction transforms a benzoid ring to a quinoid ring. The polyaniline chain upon oxidation becomes a random mixture of benzoid and quinoid rings. If the protonation of the quinoid rings decreases the self-energy of this unit significantly, the transformed problem will be a random dimer model with small ϵ_0. Since the number of nonscattered states in such a case will be quite large, a high electrical conductivity should be expected. The effect will be prominent at low temperatures and finite size samples.

The basic idea of the RDM can be employed to generate new and interesting systems. Phillips and co-workers did a great deal of work to generalize the RDM. In all cases, however, they obtained only one energy around which nonscattered states exist. We have been able to generate a system which contains two zones of nonscattered states. Similar behavior is, of course, found in the system containing randomly placed dimers of two types. The details of our model and its relevance to physical systems will be presented elsewhere.[26]

ACKNOWLEDGMENT

We greatly appreciate many useful discussions with Dr. S. M. Bhattacharjee.

* Electronic address: datta%@iopb.ernet.in
† Electronic address: giri%@iopb.ernet.in
‡ Electronic address: kundu%@iopb.ernet.in

[1] P. W. Anderson, Phys. Rev. **109**, 1492 (1958).
[2] I. M. Lifshitz, S. A. Gredeskul, and L. A. Pastur, *Introduction to the Theory of Disordered Systems* (Wiley, New York, 1988).
[3] D. Dunlap, H.-L. Wu, and P. Phillips, Phys. Rev. Lett. **65**, 88 (1990).
[4] P. Phillips, H.-L. Wu, and D. Dunlap, Mod. Phys. Lett. B **4**, 1249 (1990).
[5] H.-L. Wu and P. Phillips, Phys. Rev. Lett. **66**, 1366 (1991).
[6] P. Phillips and H.-L. Wu, Science **252**, 1805 (1991).
[7] J. Chen, A. J. Heeger, and F. Wudl, Solid State Commun. **58**, 251 (1986).
[8] D. S. Galvao, D. A. dos Santos, B. Laks, C. P. de Melo, and M. J. Caldas, Phys. Rev. Lett. **63**, 786 (1989); **65**, 527 (1990).
[9] M. Kohmoto, L. P. Kadanoff, and C. Tang, Phys. Rev. Lett. **50**, 1870 (1983).
[10] M. Kohmoto, Phys. Rev. Lett. **51**, 1198 (1983).
[11] H. Hiramoto and M. Kohmoto, Phys. Rev. B **40**, 8225 (1989).
[12] H. Hiramoto and M. Kohmoto, Phys. Rev. Lett. **62**, 2714 (1989).
[13] H. Hiramoto and M. Kohmoto, Int. J. Mod. Phys. B **6**, 281 (1992).
[14] F. Wijnands, J. Phys. A **22**, 3267 (1989).
[15] S. N. Evangelou and E. N. Economou, J. Phys. Condens. Matter **3**, 5499 (1991).
[16] H.-L. Wu, W. Goff, and P. Phillips, Phys. Rev. B **45**, 1623 (1992).
[17] A. Bovier, J. Phys. A **25**, 1021 (1992).
[18] A couple of remarks on the Lyapunov exponent will not be out of place here. The vanishing of the Lyapunov exponent at a certain energy (E) does not necessarily imply that the state at that energy is extended. The state at that energy can also be critical [M. Kohmoto, B. Sutherland, and C. Tang, Phys. Rev. B **35**, 1020 (1987)]. Furthermore, the positiveness of the Lyapunov exponent at a E does not constitute an unequivocal proof for the localization of the state (see Ref. 10). Inasmuch as the magnitude of the Lyapunov exponent is very small for energies close to the dimer energy (ϵ_0), the second statement has a tremendous significance in the present work.
[19] A. K. Sen and S. Gangopadhyay, Physica A **186**, 270 (1992).
[20] S. Gangopadhyay and A. K. Sen, J. Phys. Condens. Matter **4**, 9939 (1992).
[21] P. K. Datta, D. Giri, and K. Kundu, Phys. Rev. B **47**, 10727 (1993).
[22] P. Erdös and R. C. Herndon, Adv. Phys. **31**, 65 (1982).
[23] J. Hori, *Spectral Properties of Disordered Chain and Lattices* (Pergamon, Oxford, 1968).
[24] D. R. Grempel, S. Fishman, and R. E. Prange, Phys. Rev. Lett. **49**, 833 (1982).
[25] E. N. Economou, *Green's Functions in Quantum Physics* (Springer-Verlag, Heidelberg, 1990).
[26] D. Giri, P. K. Datta, and K. Kundu, Phys. Rev. B **48**, 14 113 (1993).